Measuring neutron star masses and radii and constraining the equation of state of nuclear matter with Constellation-X and XEUS

Mariano Méndez *(SRON)*

First Constellation-X / XEUS Science Meeting

Equation of State of nuclear matter. Neutron star mass and radius

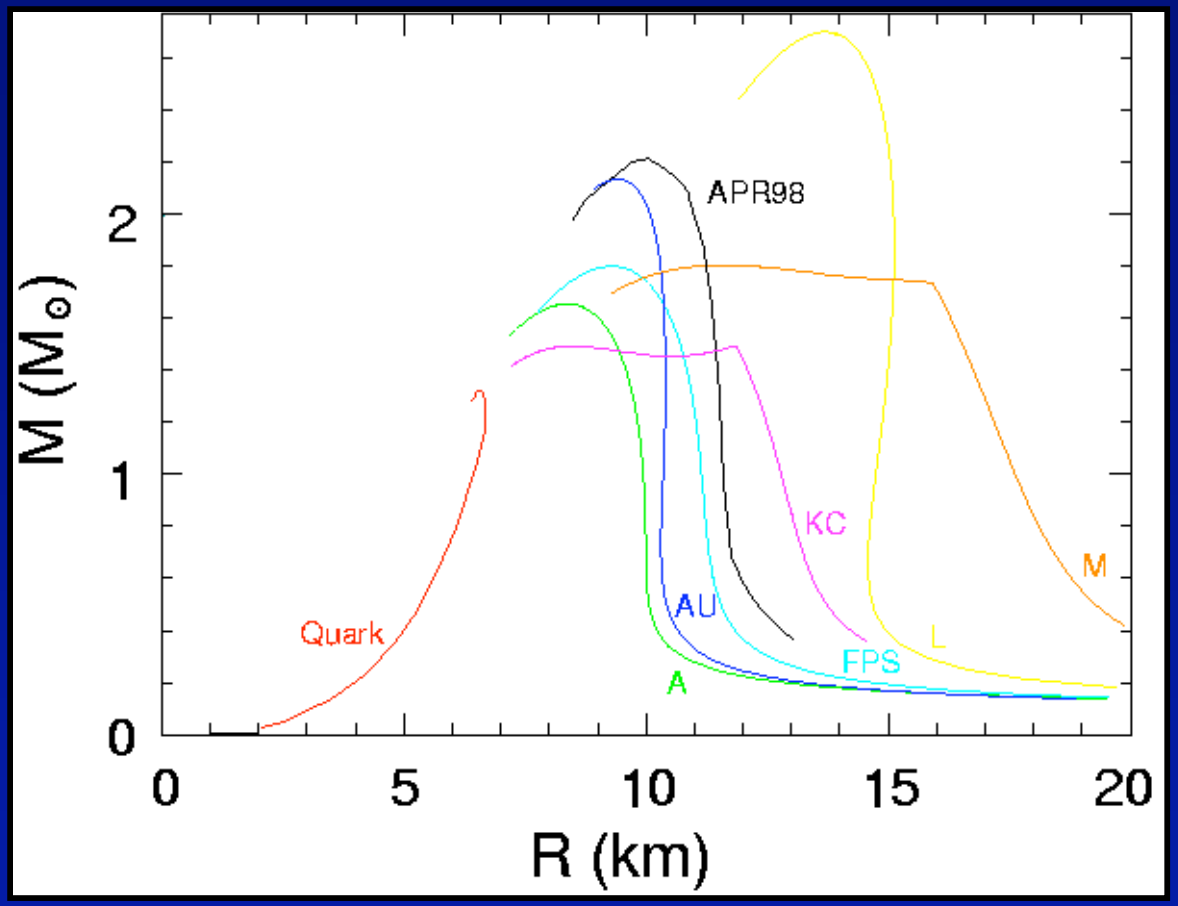

The composition of the star fixes the equation of state (the pressure-density relation), which in turns determines the structure of the star and its mass-radius relation.

This plot shows the mass-radius relation for different equations of state, with the central density varying along each curve.

Cook, Shapiro & Teukolsky 1994; Akmal,Pandharipande, Ravenhall 1998; Heiselberg 2002

If nuclear physics is correct, a measure of M and R provides the composition of the star.

Gravitational redshift

- The time dilation: $dt = (-g_{00})^{-1/2}\,\Delta t$

  $g_{\mu\nu}$: metric tensor,

  Δt : the proper time in the gravitational field,

  dt : time measured by an observer at infinity,

which in the Schwarzschild's metric yields:

$$\frac{\Delta t}{dt} = \left(1 - \frac{2M\,G}{c^2\,R}\right)^{1/2} = \frac{\nu}{\nu_0} = \frac{\lambda_0}{\lambda}$$

From a measurement of the gravitational redshift, $z = \Delta\lambda/\lambda$, we can infer the compactness (M/R) of the neutron star:

$$\frac{M}{R} = \frac{c^2}{2G}\left[1 - (1+z)^{-2}\right]$$

Photospheric absorption during X-ray bursts

EXO 0748–676, a known X-ray burster

XMM-Newton observed it as a calibration target:

~ 335 ks with RGS cameras; 28 X-ray bursts.

~ 39 ks with EPIC simultaneous.

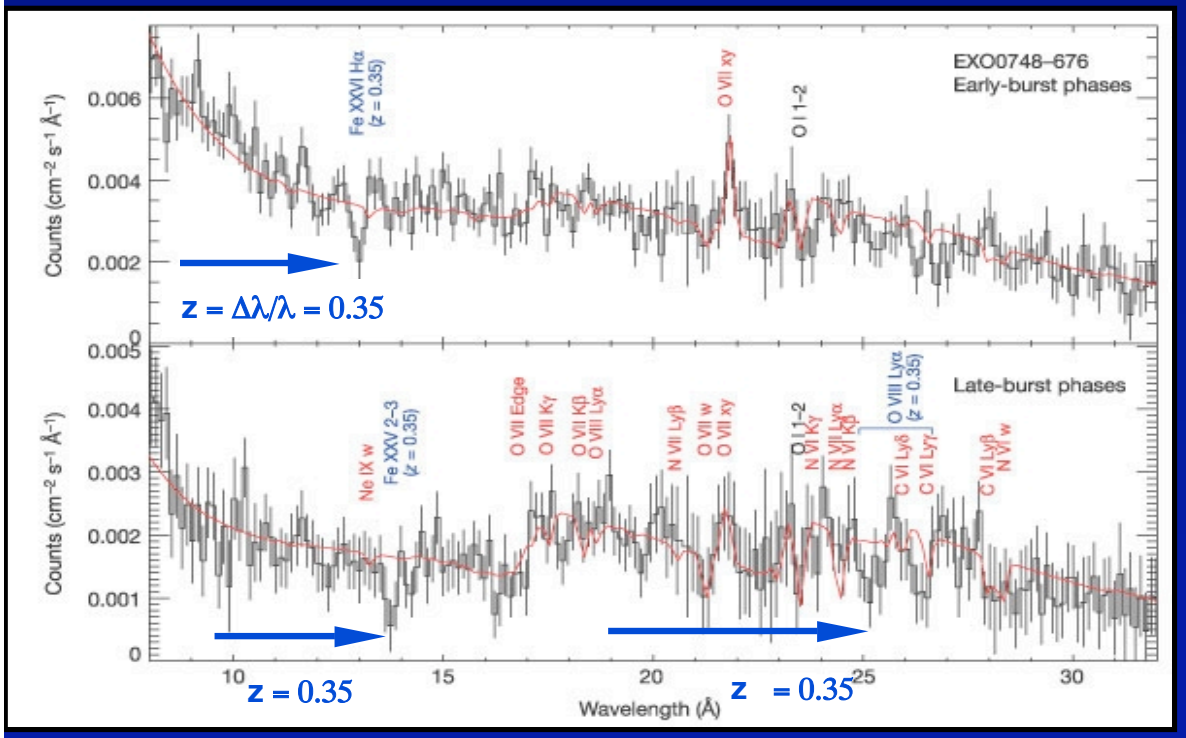

Absorption lines at λ13.0Å and λ13.7Å in the combined early- and late-burst spectra, respectively.

Consistent with FeXXVI Hα (n = 2–3) and FeXXV Heα (n = 2–3), respectively, both at the same redshift $z = 0.350 \pm 0.005$.

The feature at λ25.3 Å in the late-burst spectrum would then be consistent with OVIII Lyα.

Cottam, Paerels & Mendez 2003

EOS – Constraining mass and radius

$\frac{M}{R} = 0.153\ M_{\odot}/\mathrm{km}$

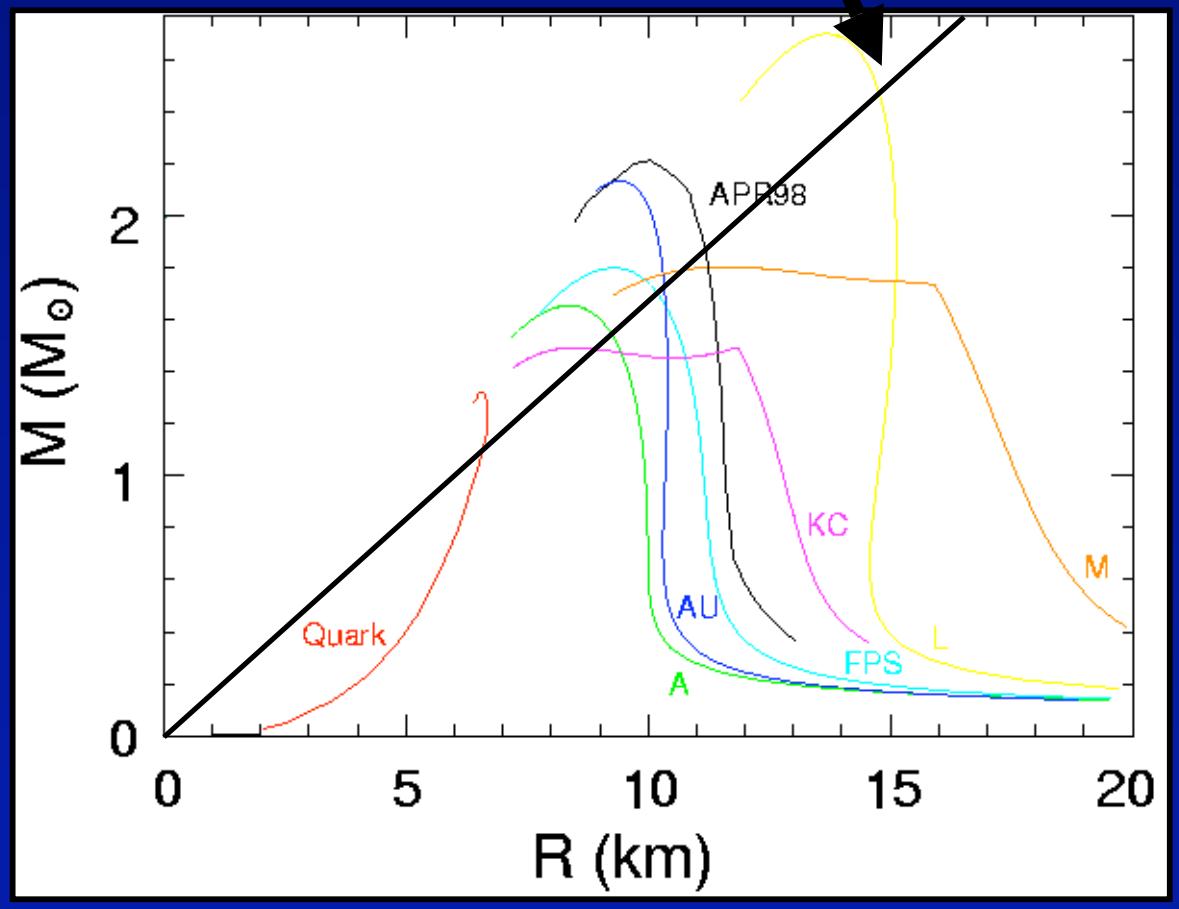

Cottam, Paerels & Mendez 2003

Dynamical constraints of the masses.

Masses of NS obtained from pulsars in binary systems.

$< M > = 1.35 \pm 0.04\ M_{\odot}$

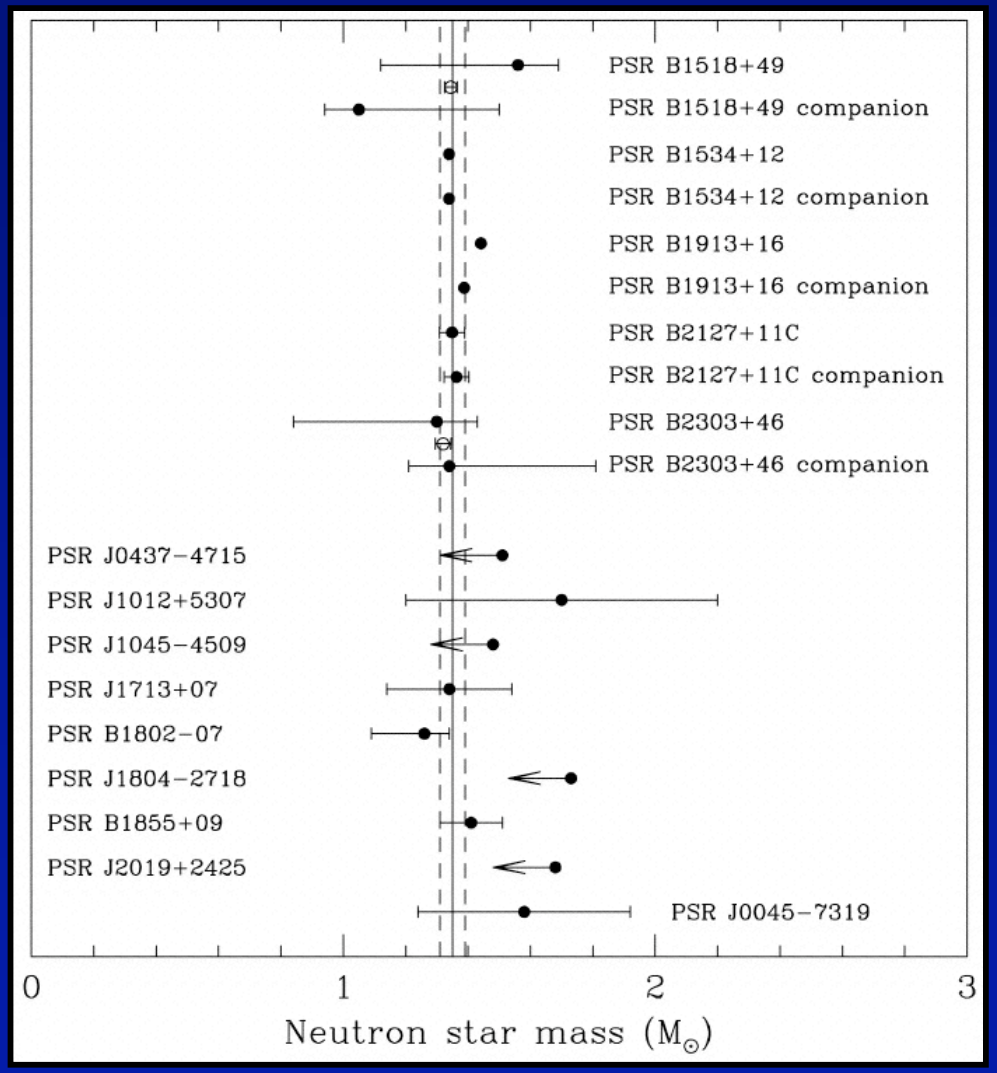

Thorsett & Chakrabarty 1999

EOS – Constraining mass and radius

$\frac{M}{R} = 0.153 \pm 0.001\ M_\odot/km$

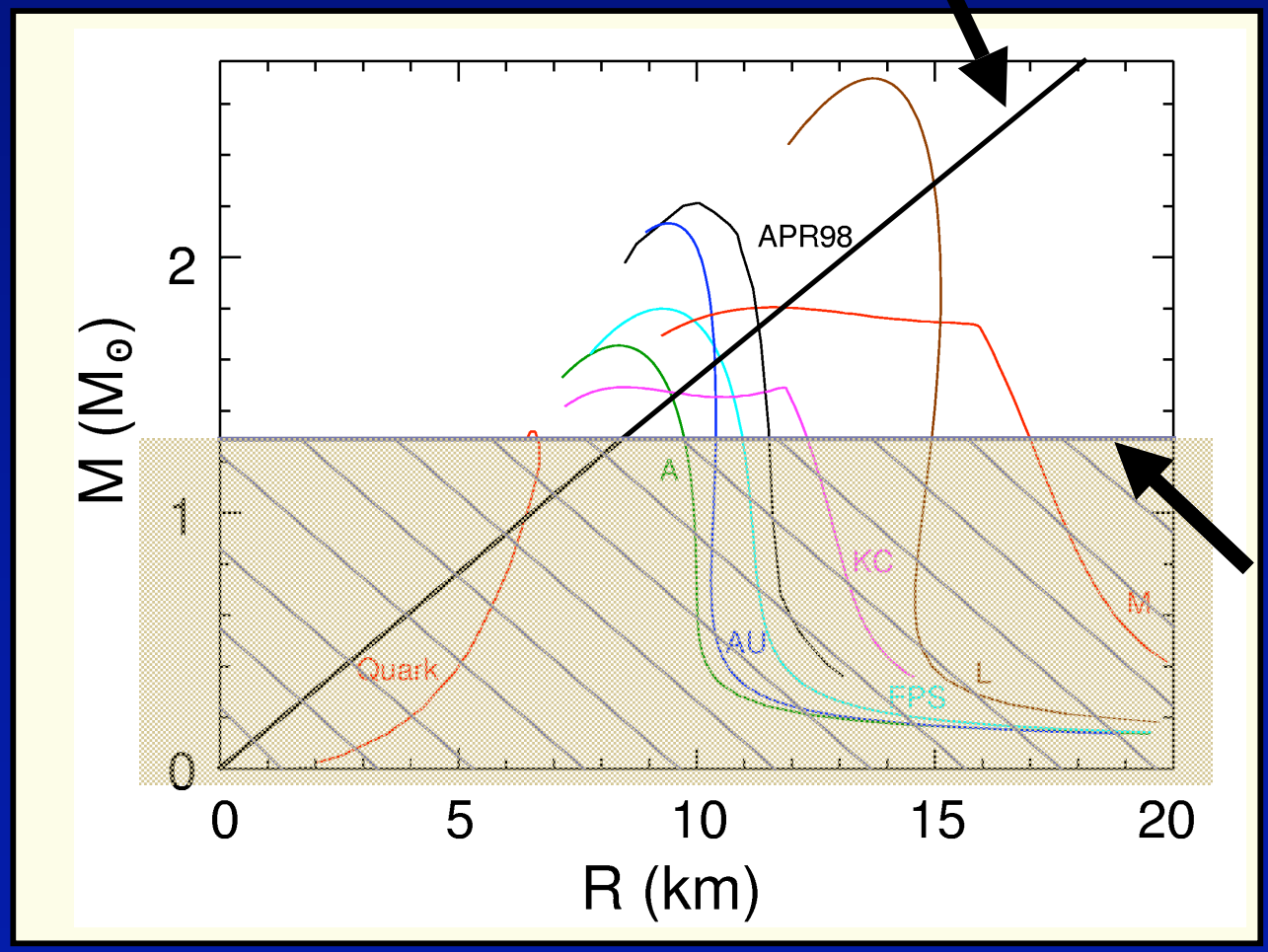

$M \sim 1.3\ M_\odot$

Constraints from timing

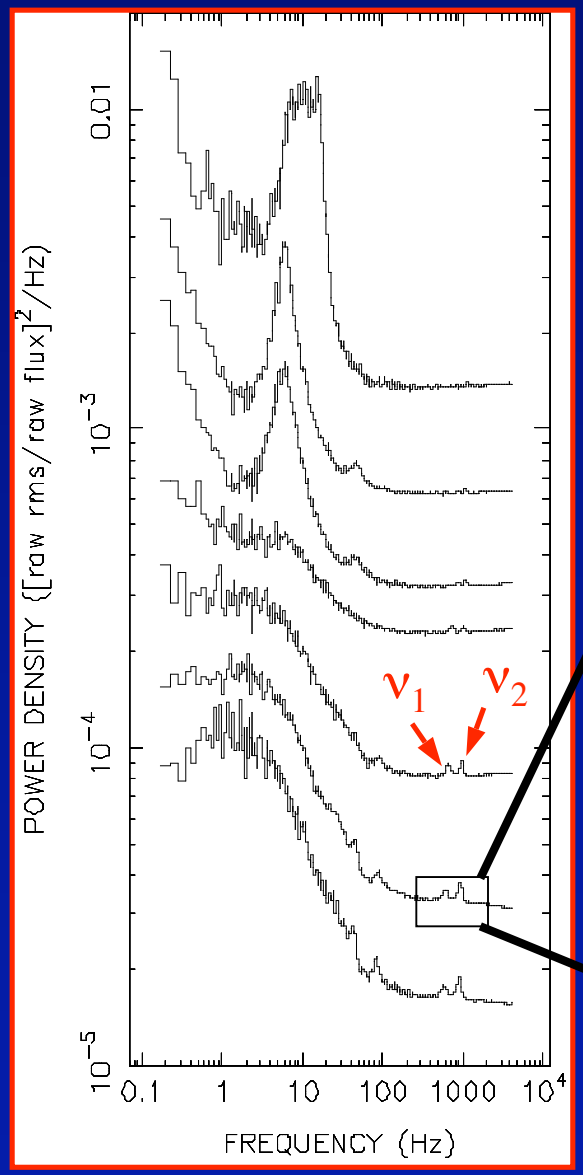

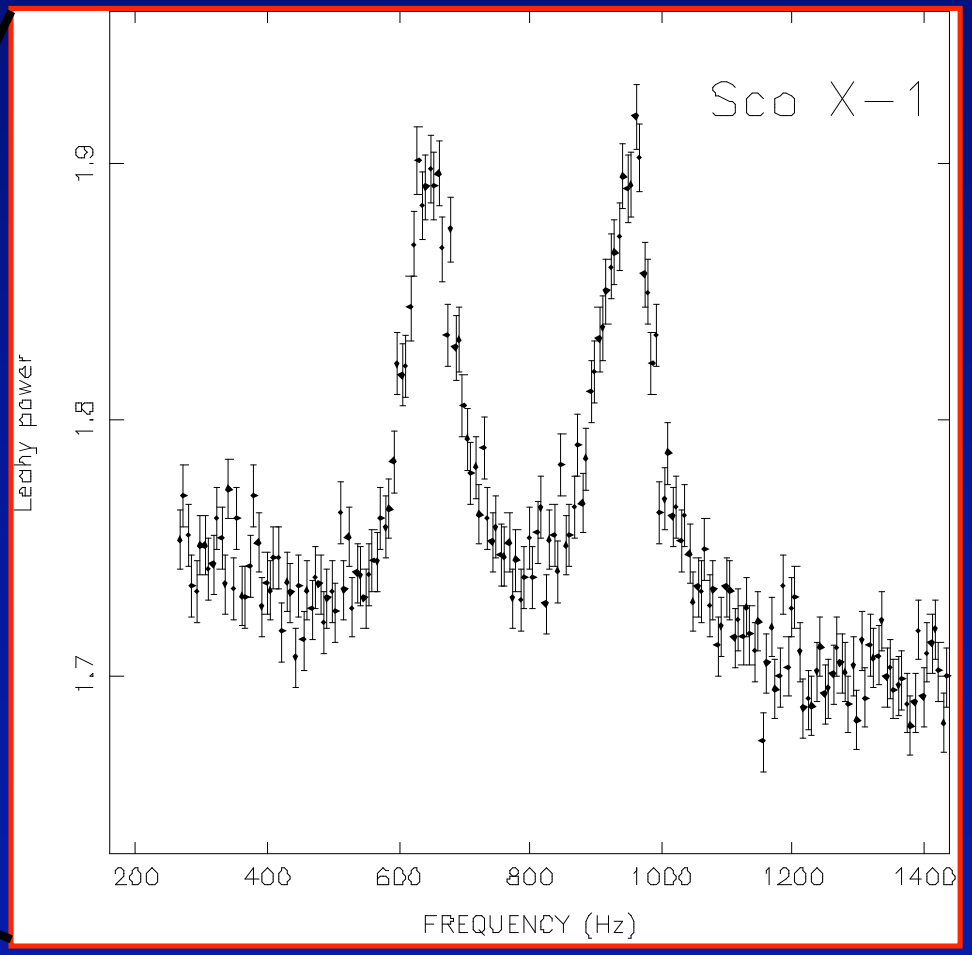

van der Klis et al. 1997

Innermost Stable Circular Orbit

Effective potential $V_{eff} = V(R) + \frac{l^2}{2mR^2}$

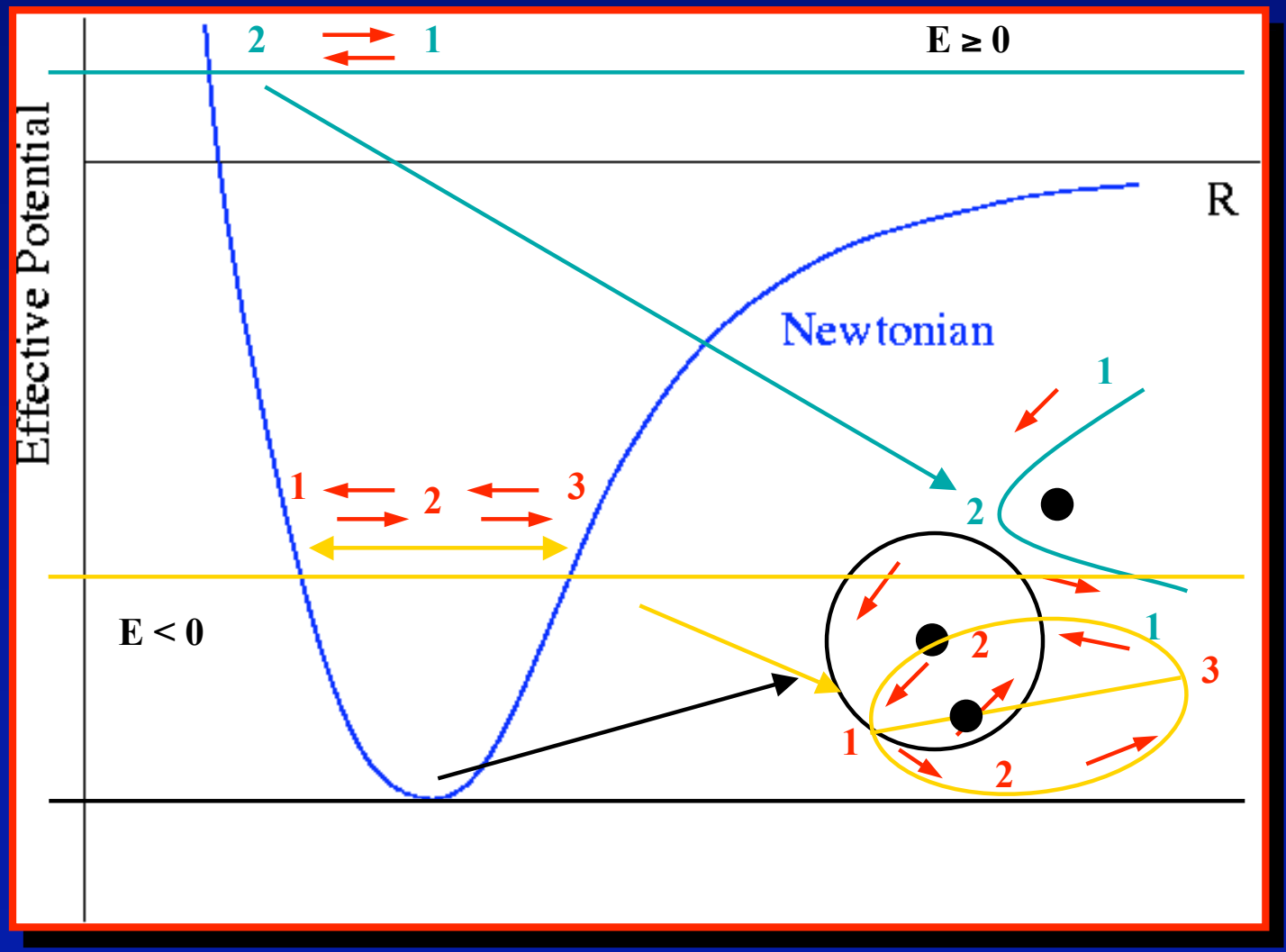

Innermost Stable Circular Orbit

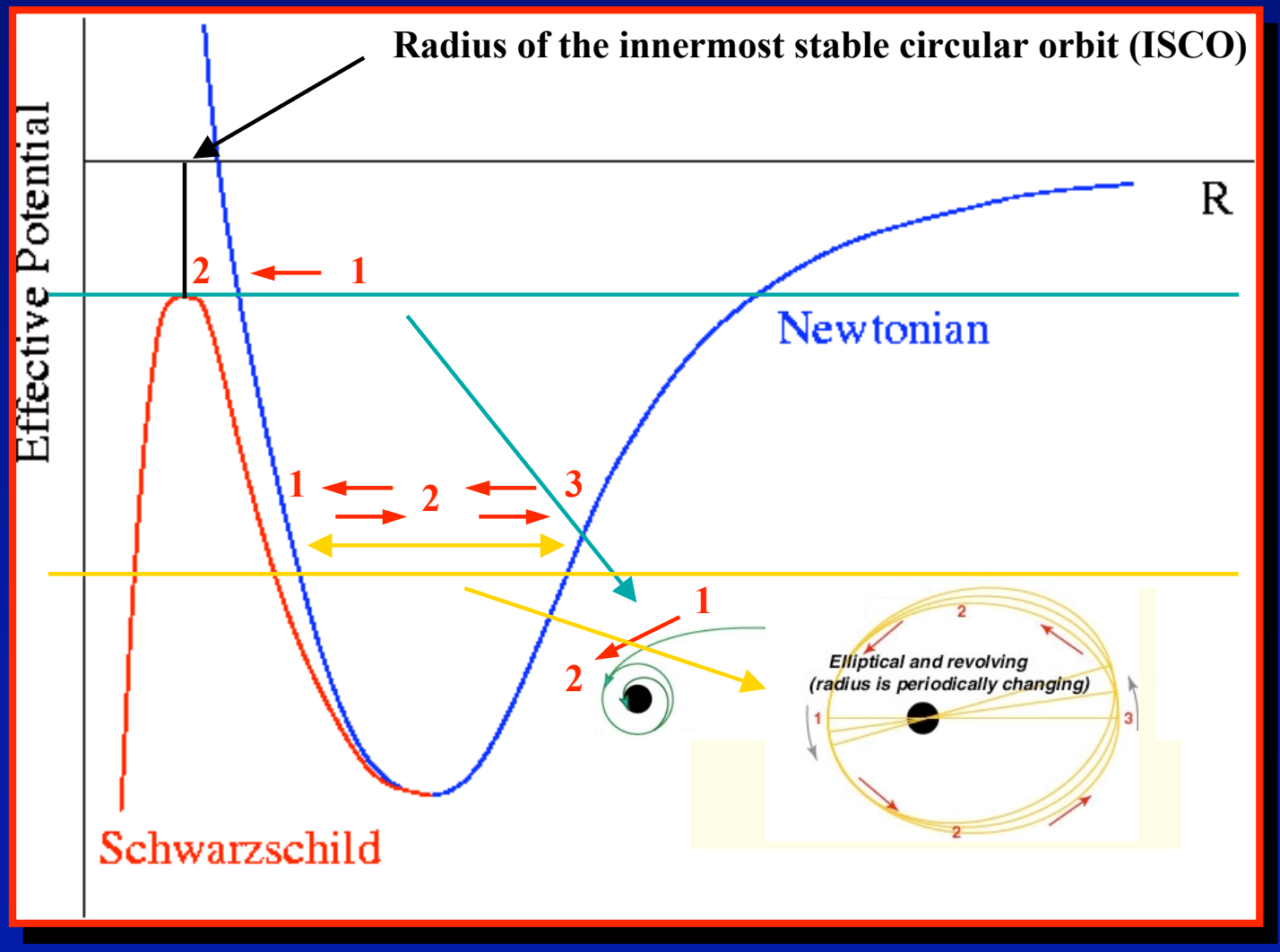

Innermost Stable Circular Orbit

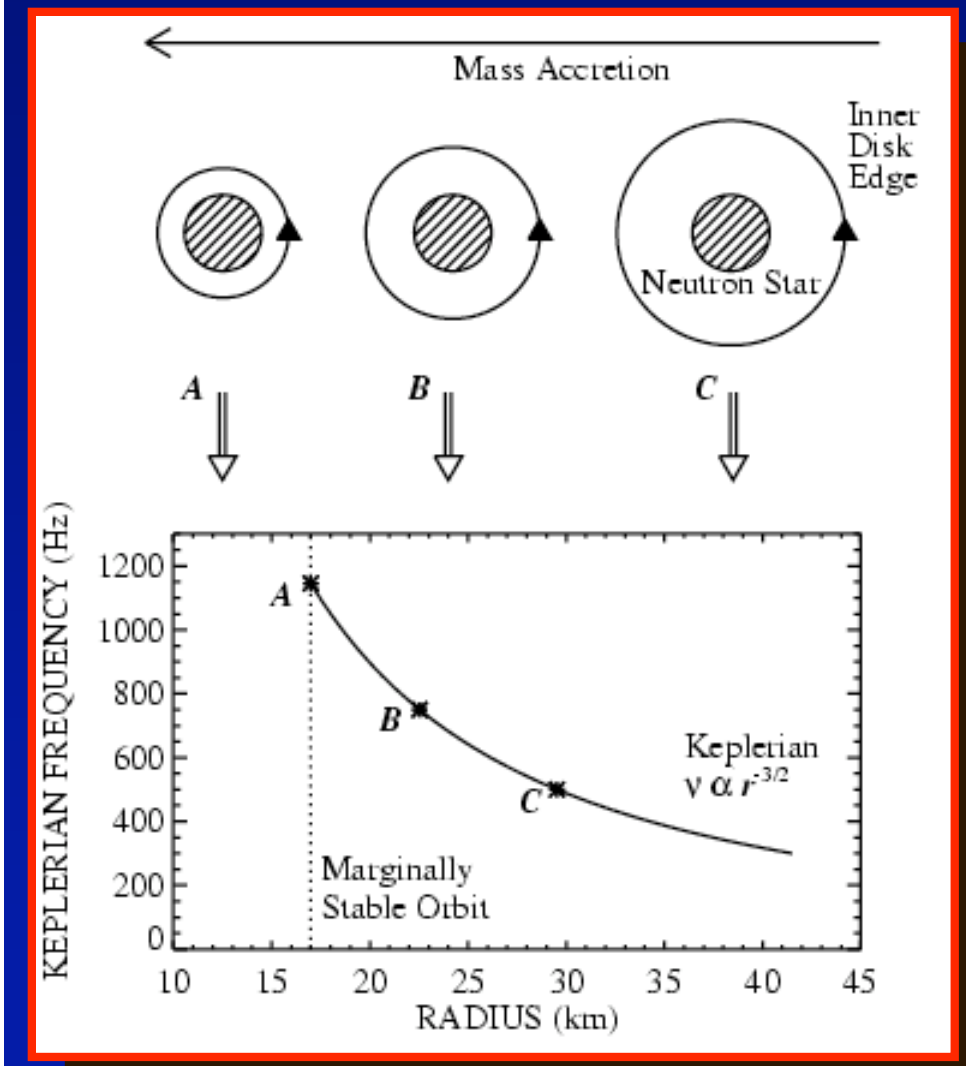

As the radius of the inner edge of the accretion disk decreases, probably driven by mass accretion rate onto the neutron star, the orbital frequency at that radius (probably the frequency of the high-frequency QPO ; see talk by Didier Barret) increases.

But this frequency cannot be higher than the Keplerian frequency at the ISCO.

Mass and radius constraints from timing

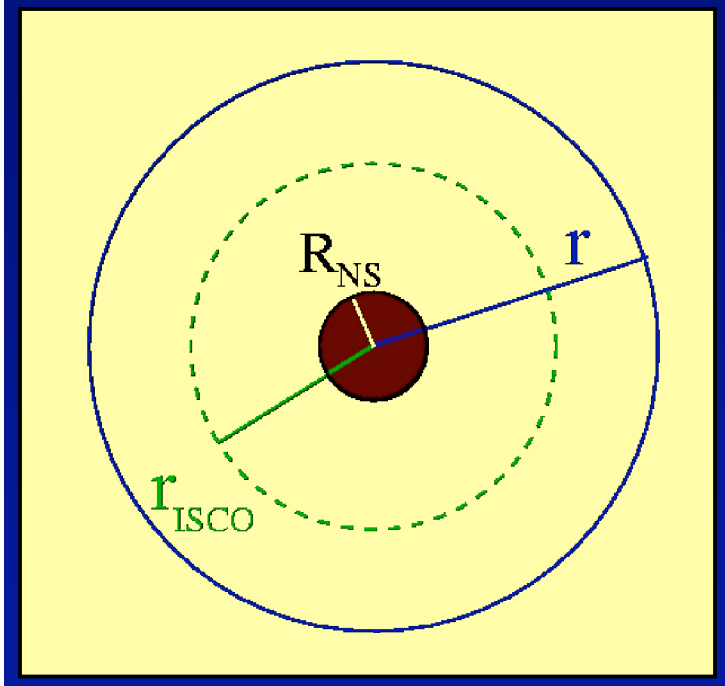

$\nu = 1/(2\pi)\ (G\ M_{NS}\ r^{-3})^{1/2}$

$r_{ISCO} \leq r$

$R_{NS} \leq r$

$r_{ISCO} = 6\ G\ M_{NS}/c^2$

(Schwarzschild ≡ non-rotating NS)

$M_{NS} \leq 2.2\ (\nu/1000\ \mathrm{Hz})^{-1}\ M_{\odot}$

$R_{NS} \leq 14.6\ (M_{NS}/M_{\odot})^{1/3}\ (\nu/1000\ \mathrm{Hz})^{-2/3}\ \mathrm{km}$

Mass and radius constraints from timing

$M_{NS} \leq 2.2\ (\nu/1000\ \mathrm{Hz})^{-1}\ M_{\odot}$

For $\nu = 1329$ Hz

$R_{NS} \leq 14.6\ (M_{NS}/M_{\odot})^{1/3}\ (\nu/1000\ \mathrm{Hz})^{-2/3}$ km

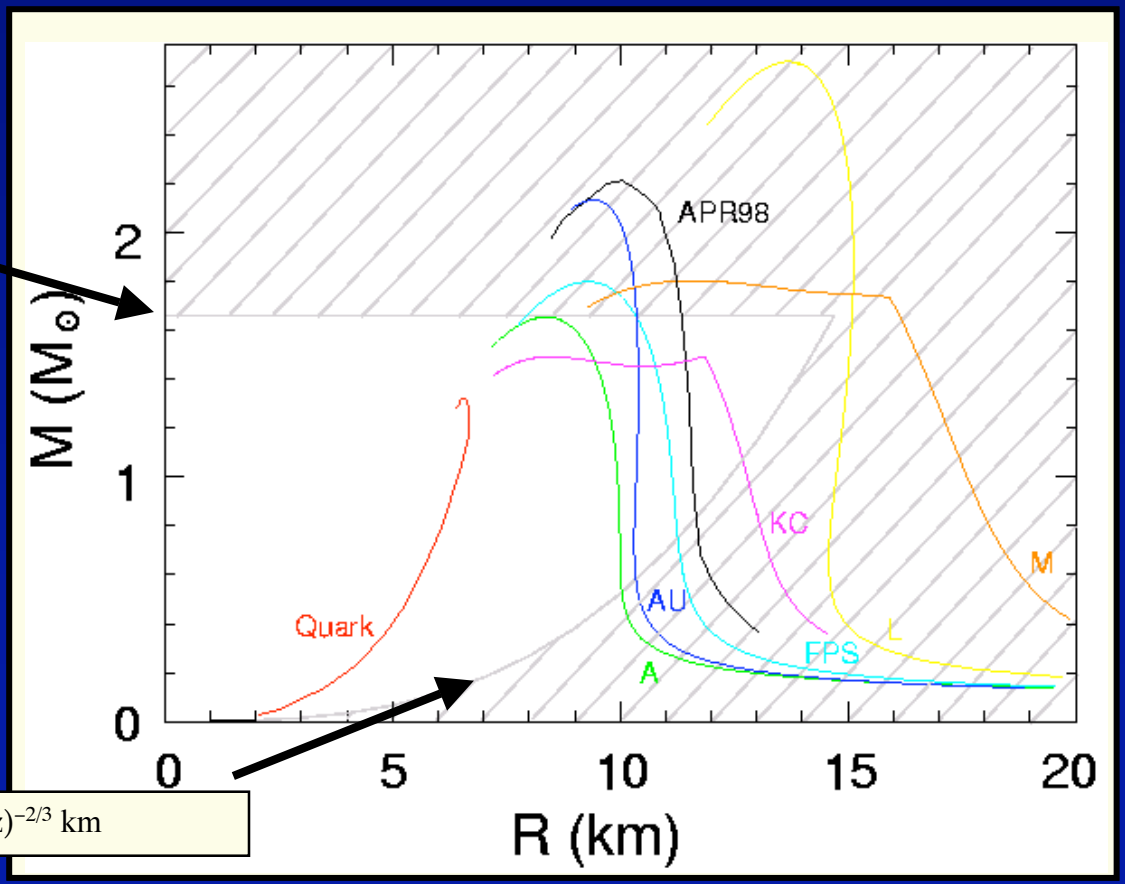

Miller et al. 1998; van Straaten et al. 2000

EOS – Combined constraints

$\frac{M}{R} = 0.153 \pm 0.001\ M_\odot/km$

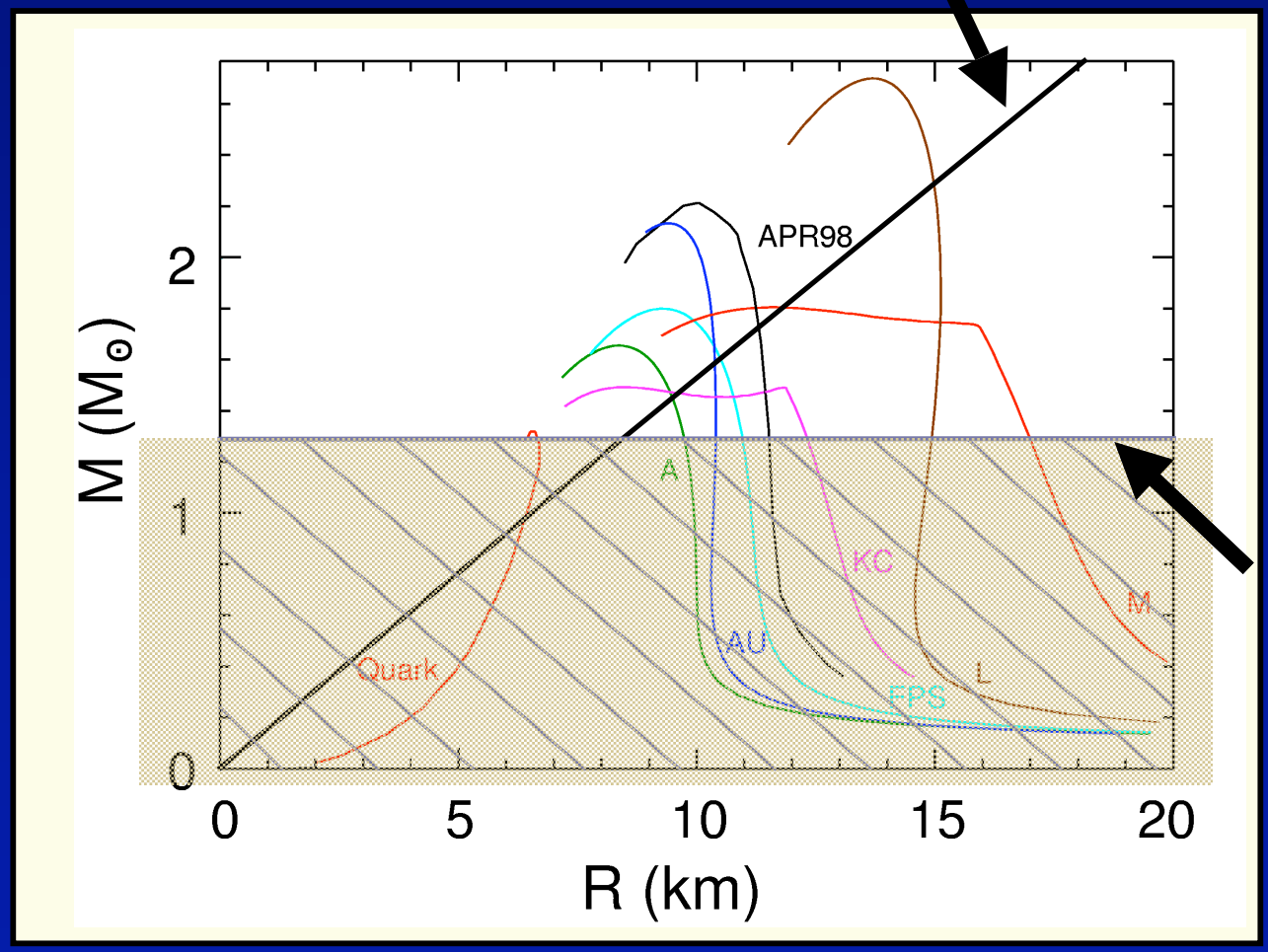

$M \sim 1.3\ M_\odot$

EOS – Combined constraints

$R \leq 14.6\ (M / M_\odot)^{1/3}\ (\nu/1000\ \mathrm{Hz})^{-2/3}$ km

$\frac{M}{R} = 0.153 \pm 0.001\ M_\odot/\mathrm{km}$

$M \leq 2.2\ (\nu/1000\ \mathrm{Hz})^{-1}\ M_\odot$

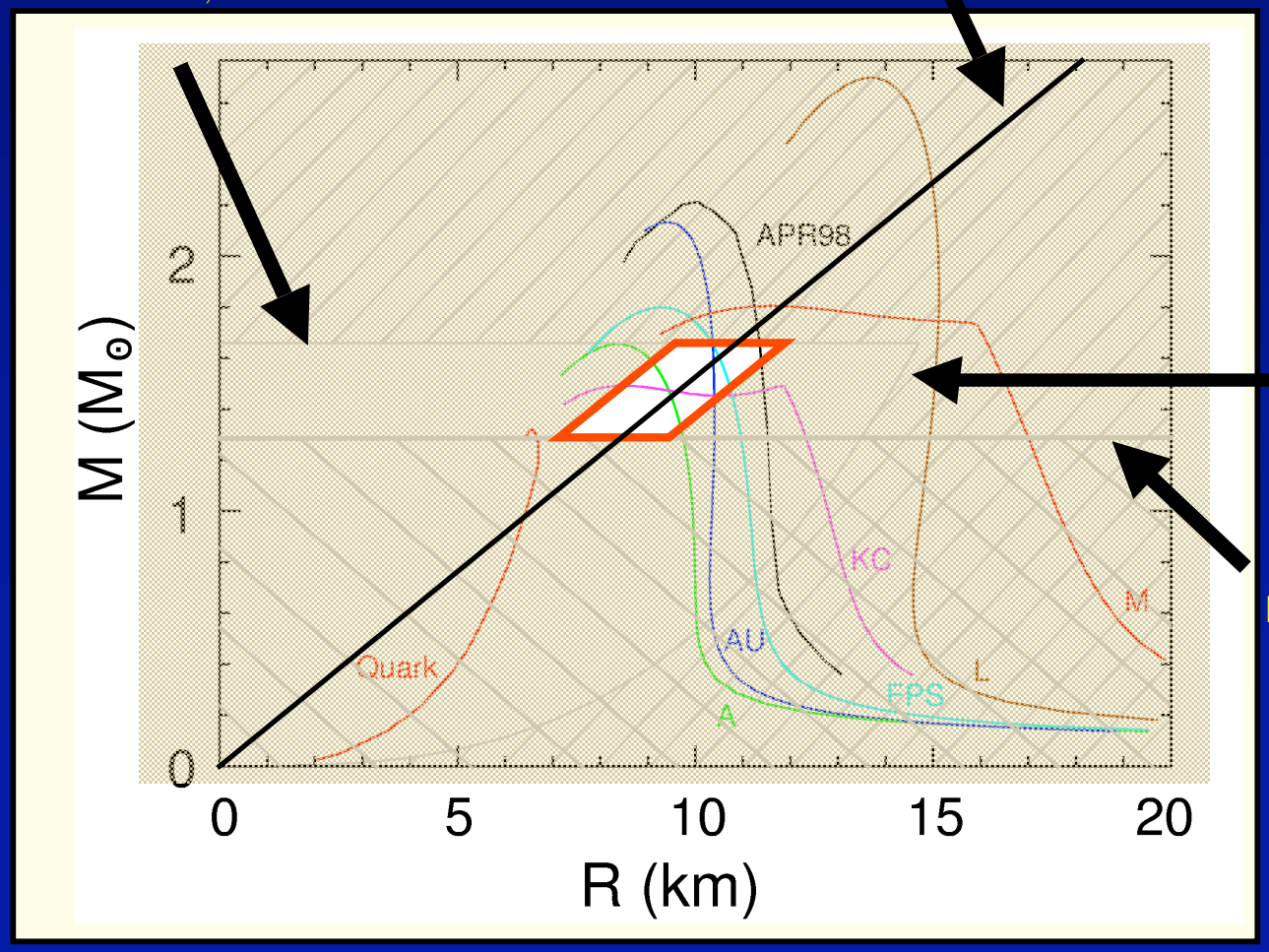

$M \sim 1.3\ M_\odot$

Burst spectra: simulations

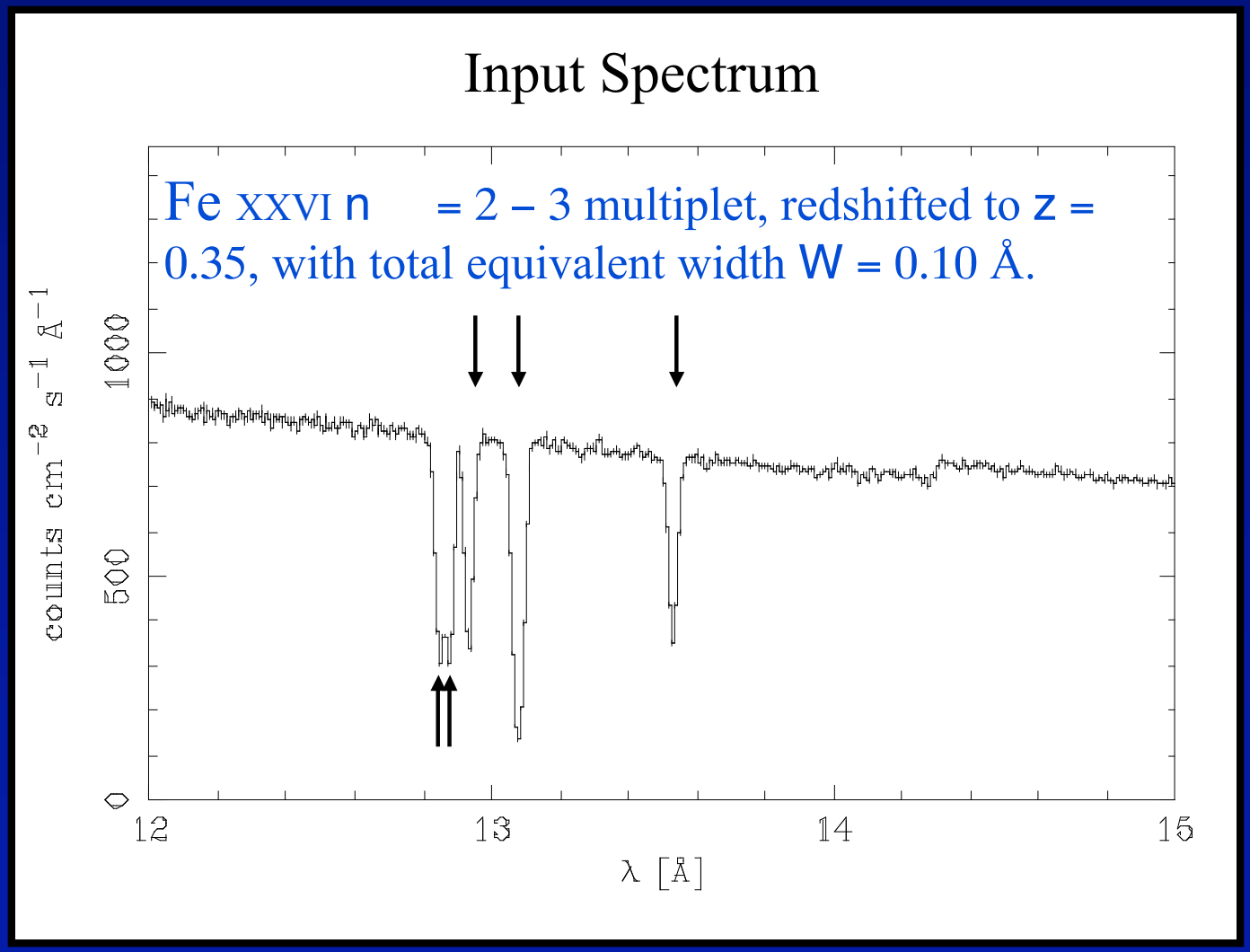

Burst spectra: simulations

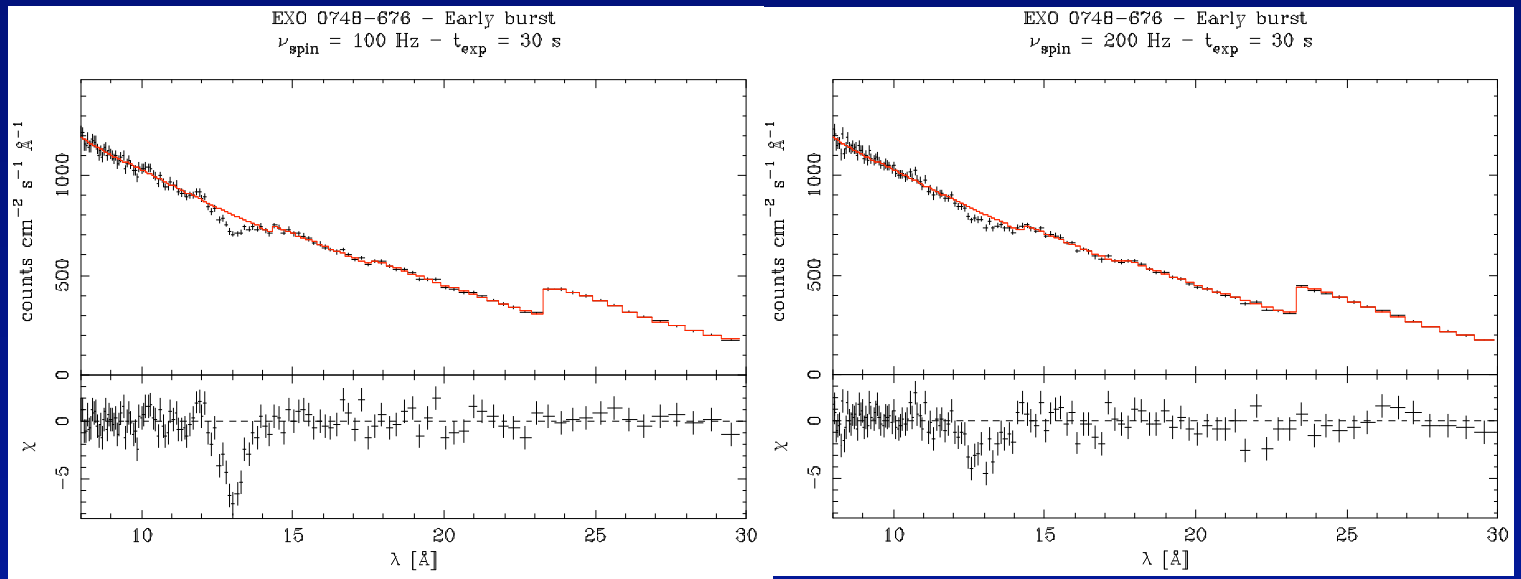

30-second exposures of the early part of a single X-ray burst, for 3 different spin frequencies of the neutron star, and 10-m^2 X-ray detector with a 5-eV spectral resolution.

Resolving the multiplet

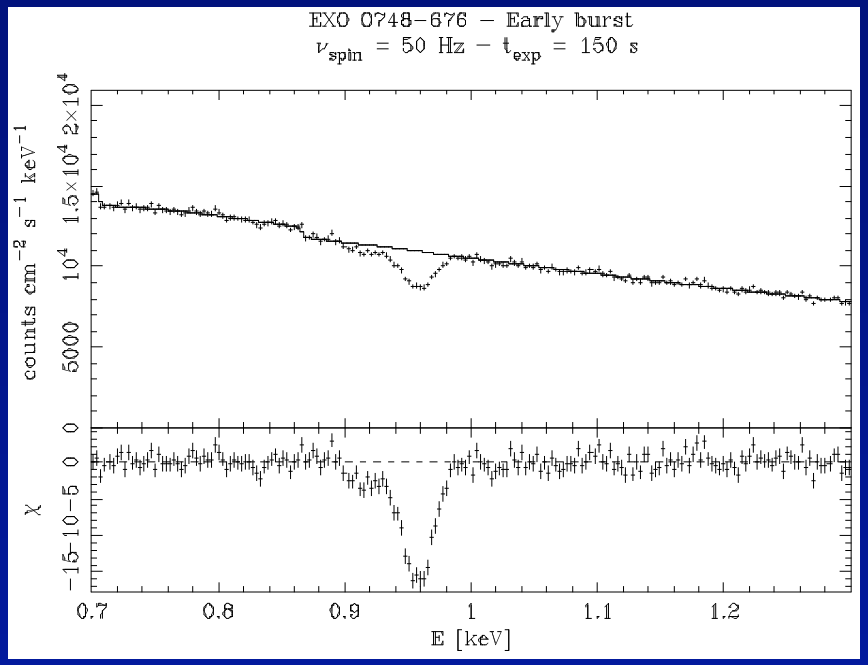

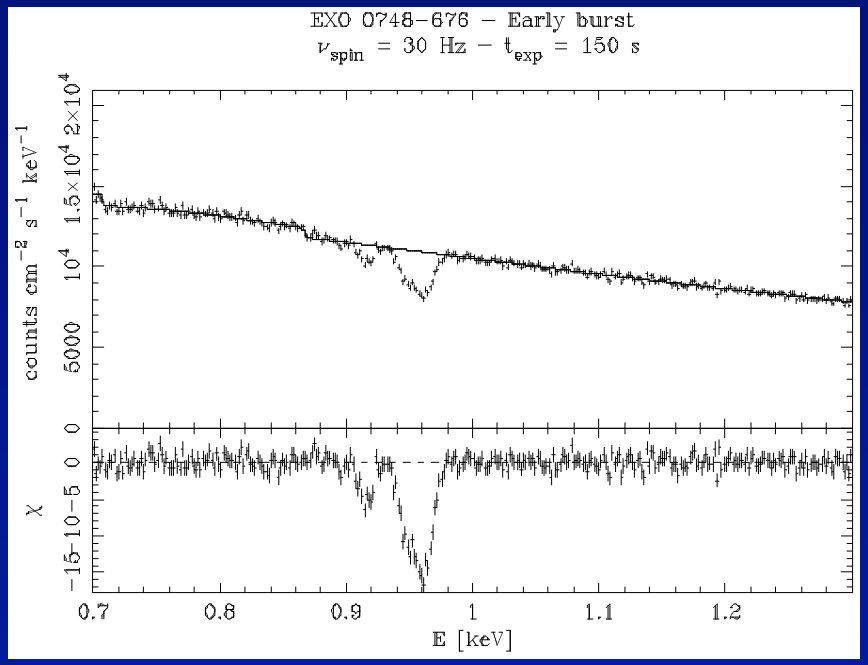

150-second exposures (~5 bursts co-added) of the early part of the bursts, for 2 different spin frequencies of the neutron star (slow rotator). Again, a 10-m^2 X-ray detector with a 5-eV spectral resolution has been used for the simulations.

Observing with / without gratings

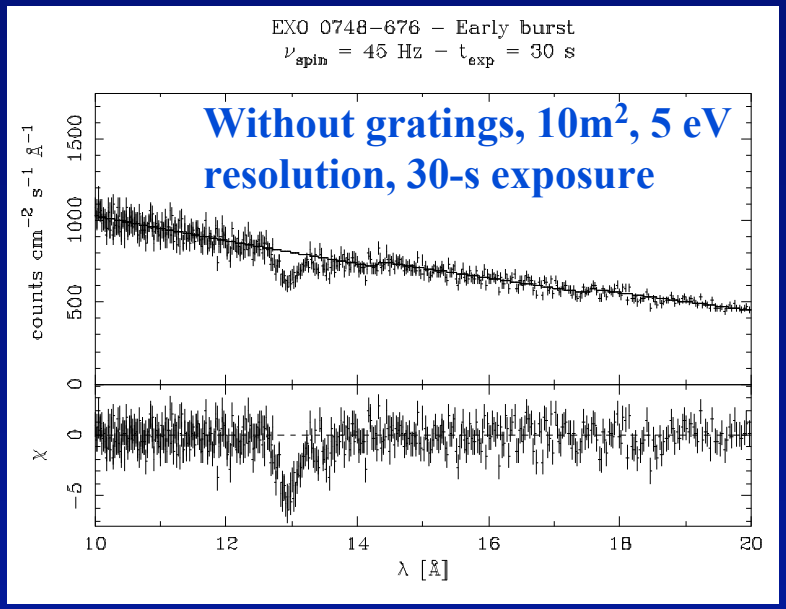

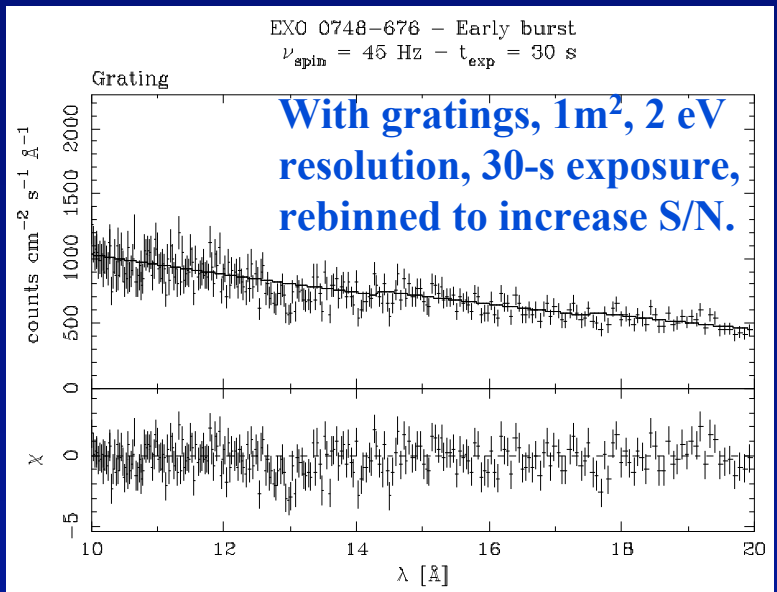

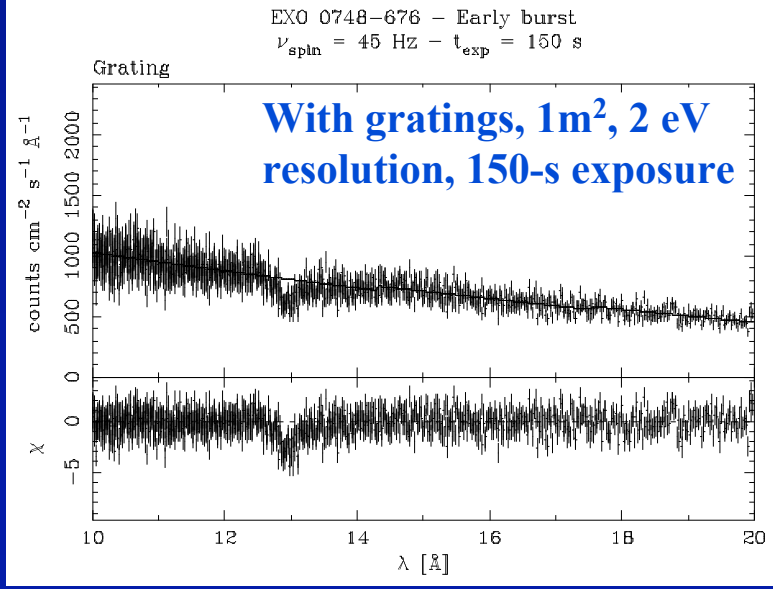

The reduced effective area of the gratings (here assumed to be 10% of the main 10-m^2 mirror) makes it impossible to detect lines within a single burst. Finer spectral resolution does not provide a gain since lines are intrinsically broad.

Mass and radius constraints from X-ray spectroscopy: Line broadening and equivalent width.

The equivalent width of the Fe line in EXO 0748–676 at 13Å is $W_\nu / \nu = 0.01$.

Assuming only thermal (Doppler) broadening, the expected equivalent width of the line would be:

$$W_\nu \_ 4 \times 10^{12} \, (x_i / 0.5)^{1/2} \, (A_{Fe} / A_{Fe,/})^{1/2} \ \text{Hz},$$

with x_i the fraction of the ions in the relevant excited state, and A_{Fe} the iron abundance in the neutron star atmosphere.

Line broadening and equivalent width

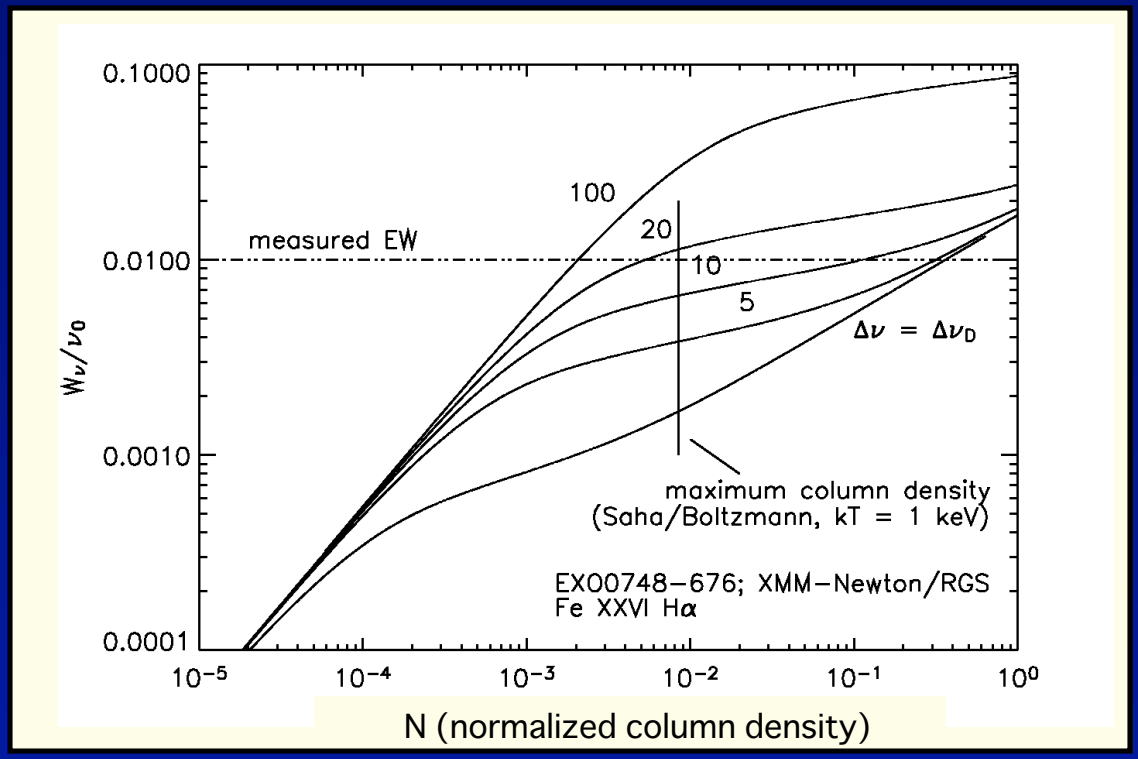

Curve of growth for Fe XXVI $n = 2 - 3$ transition. The lower curve is for thermal broadening alone, assuming solar Fe abundance. The other curves show additional broadening of 5, 10, 20, and 100 times the thermal width. The vertical line indicates the column density in case the fraction of ions of Fe XXVI at level $n = 2$, is unity. The horizontal dashed line is the measured equivalent width.

The measured equivalent width of the line, $(W_\nu/\nu_0) = 0.01$, is about an order of magnitude larger than thermal broadening alone.

Either Fe abundance is ~100 times solar ($W_\nu \propto A_{Fe}^{1/2}$), or another mechanism is responsible for the line broadening. (Notice that the equivalent width is independent of the spin frequency of the neutron star.)

Line broadening and equivalent width

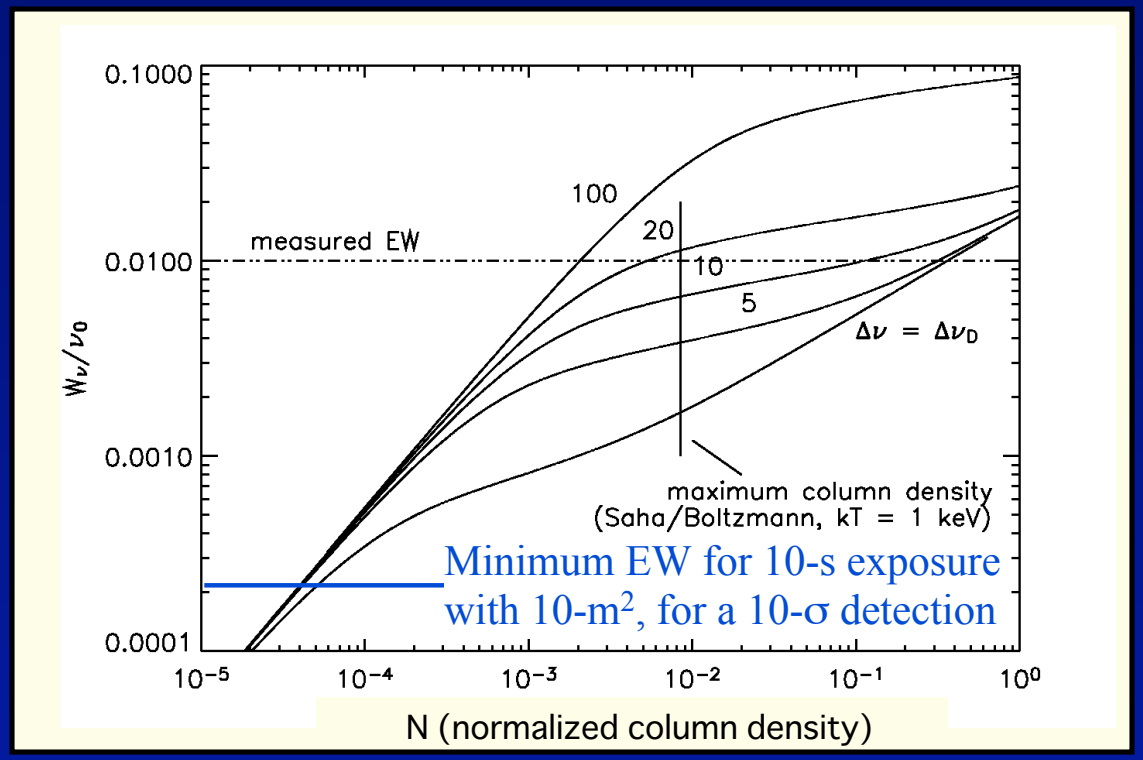

Curve of growth for Fe XXVI $n = 2 – 3$ transition. The lower curve is for thermal broadening alone, assuming solar Fe abundance. The other curves show additional broadening of 5, 10, 20, and 100 times the thermal width. The vertical line indicates the column density in case the fraction of ions of Fe XXVI at level $n = 2$, is unity. The horizontal dashed line is the measured equivalent width.

Stark effect would broaden the line by:

$$\Delta E \approx (160 / Z)\,(M/1.4\,M_\odot)^{2/3}\,(R/10\ \mathrm{km})^{-4/3}\,(T/10^6\ \mathrm{K})^{-2/3}\,n\,(n-1)\ \mathrm{eV},$$

with Z the nuclear charge, and n the quantum number of the upper level of the transition. For typical values $\Delta E \approx 10$ eV, and $(W_\nu/\nu_0)_{\mathrm{Stark}} \approx 0.01$, as observed.

Paerels 1997

Other lines

Extrapolating from the original EXO 0748–676 results.

Fe XXVI Lyman series (n = 1 – m): The redshifted Fe XXVI n = 1 – 2 line will appear at E = 5.165 keV, and will have a maximum equivalent width W » 30 eV (high-energy response would be needed to constrain the continuum).

Fe XXVI Balmer series (n = 2 – m): The redshifted Fe XXVI n = 2 – 4 line will appear at λ = 9.65 Å and will have an equivalent width W » 0.03 Å.

Fe XXVI Paschen series (n = 3 – m): The n = 3 – 5 line will be at λ = 25.6 Å, and will have an equivalent width W » 0.2 Å. The n = 3 – 6 line will be at λ = 21.8 Å and will have an equivalent width W » 0.1 Å.

Effect of a weak magnetic field

1. A relatively low magnetic field induces Zeeman splitting of an atomic level with an energy separation that is linear in the field strength:

$$\Delta E_{split} = (eh/4\pi m_e c)(M_L + 2M_S) B = 11.6 \text{ eV } (B/10^9 \text{ G}),$$

where M_L and M_S are the angular momentum and spin quantum numbers.

2. A strong magnetic field produces a net blueshift of the line centroid. For H-like atoms:

$$\Delta E_{shift} = (e^2 a_0^2/8Z^2 m_e c^2) n^4 (1+M_L^2) B^2$$

$$= 9.2 \times 10^{-4} \text{ eV } (Z/26)^{-2} n^4 (1+M_L^2) (B/10^9 \text{ G})^2,$$

with n the principal quantum number of the upper level, a_0 the Bohr radius, and Z the atomic charge.

Loeb 2003

Effect of a weak magnetic field

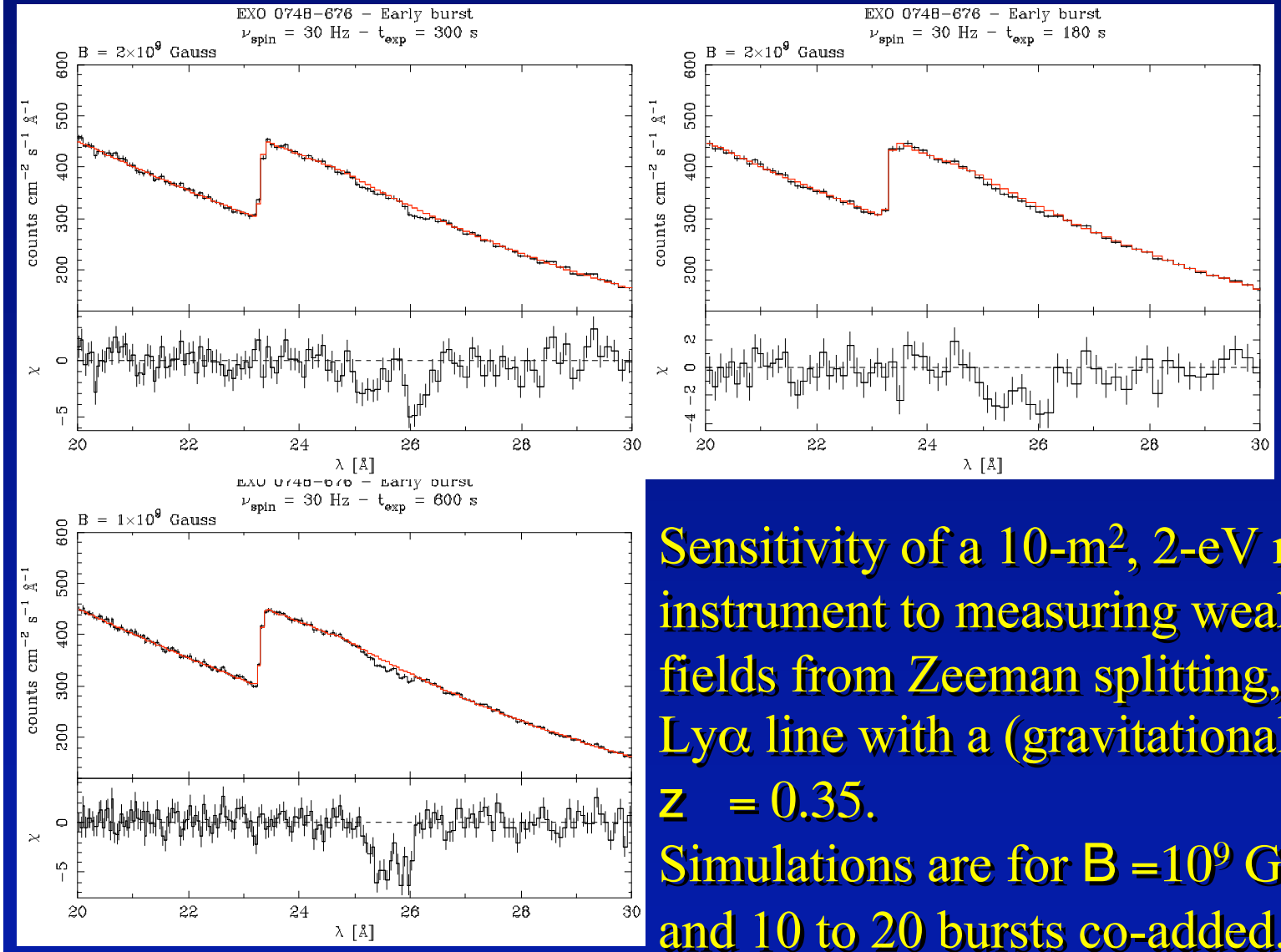

Sensitivity of a 10-m^2, 2-eV resolution, instrument to measuring weak magnetic fields from Zeeman splitting, for the OVIII Lyα line with a (gravitational) redshift z = 0.35.

Simulations are for B =10^9 G and 2£10^9 G and 10 to 20 bursts co-added.

Critical capabilities: 1. Spectroscopy

- Angular resolution: Not a driver
  ~10^{00} to avoid confusion.
- Field of view: Not a driver
  Point-like sources.
- Band pass: ~0.3 keV – 12 keV (~1 Å – 30 Å)
  Lower bound to detect high-order Paschen lines.
  Upper bound to constrain continuum around Fe Lyα.
- Spectral resolution: ~3 eV at 1 keV
  For typical rotational/pressure broadening.
- Effective area: As large as possible.
  At least 10 m^2 for single-burst line detection
  (for slow/moderate rotators).
- Max. count rate: ~10^5 counts/s during 1–5 s (burst peak).
  Pile-up may be a problem. Defocusing?
- Time resolution: Not a driver.

Critical capabilities: 2. Timing

- Angular resolution: Not a driver
  ~10^{00} to avoid confusion.
- Field of view: Not a driver
  Point-like sources.
- Band pass: ~1 keV – 25 keV (~ 0.5 Å – 12 Å)
  Amplitude of variability increases with energy.
- Spectral resolution: Not a driver
  Some spectral information, ΔE/E _ 10%, desirable.
- Effective area: As large as possible.
  See talk by Didier Barret.
- Max. count rate: ~5 £ 10^6 counts/s (see Didier Barret's talk).
  Pile-up may be a problem. Defocusing?
- Time resolution: τ ~ 10 μs or less.